Direct differential-cross-section calculations for ion-atom and atom-atom collisions in the keV range

R. Cabrera-Trujillo, J. R. Sabin, Y. Öhrn, and E. Deumens
Quantum Theory Project, Department of Chemistry and Department of Physics, University of Florida, Gainesville, Florida 32611-8435
(Received 11 August 1999; published 16 February 2000)

The direct differential cross section and the total cross section for scattering of 0.5-, 1.5-, and 5.0-keV H^+, H, and He projectiles by He and Ne targets over the laboratory scattering angle range $0.01° - 10.0°$ are studied using the electron nuclear dynamics theory, which treats the simultaneous dynamics of all electrons and nuclei. Emphasis is put on the quantum effects of the forward peak scattering. Comparison of the present results with available experimental data shows very good agreement.

PACS number(s): 34.50.−s

I. INTRODUCTION

The detailed understanding of basic atomic and molecular collision processes is of fundamental physical interest and plays an important role in a wide range of research areas as, for example, plasma physics, stopping power, and radiology to mention but a few. Over the years many theoretical approaches have been formulated and implemented in detail to study ion-atom collisions. Some of the theoretical methods for studying dynamics in a collision are (a) *T*-matrix calculation for a particular channel [1], (b) the unified atomic orbital-molecular orbital (AO-MO) matching method [2], (c) the multiple scattering method with a continuum distorted-wave approximation [3], (d) the MO expansion method with electron translation factors (ETF's) [4], (e) differential and integrated density matrix calculation for a particular channel [5], (f) the AO close-coupling method [6–10], (g) the eikonal approximation [11], (h) single-channel potential scattering [12], (i) the direct solution of the time-dependent Schrödinger equation using atomic [13] and molecular basis function [14], (j) the lattice method [15,16] which is based on the discretization of the operators and wave function on a spatial Cartesian grid, (k) the time-dependent fluid density functional method [17,18], (l) the Car-Parrinello method [19–21], (m) the time-dependent density functional method [22], (n) the direct solution of the time-dependent Hartree-Fock equations [23–25], and (o) the time-dependent variational method [26]. For a more detailed description of all the models for time-dependent dynamics, we refer the reader to the work of Deumens *et. al* [26]. Most of all the above studies adopt an impulse approximation, i.e., a straight-line trajectory for the projectile. These kind of methods are not suited to study angular processes, and up to now, they have been only applied to small system such as proton on atomic hydrogenic systems. With respect to the time-dependent Hartree-Fock theory there has been some implementation which consider the rearrangement of the constituents based on expansions in molecular or atomic state basis [27], however, they assumed a rotating frame in cylindrical coordinates which introduces a Coriolis term which couples states having *m* values which differ by one unit.

To avoid the above mentioned problem, we use the electron-nuclear dynamics (END) formalism [26,28–31], which is a time-dependent treatment of all electrons and nuclei. The current implementation of the END theory describes the electrons with a family of complex, spin unrestricted, single determinantal wave functions and the nuclei as classical particles, but no restrictions are placed on the electron nuclear coupling, which means that the description of the dynamics is fully nonadiabatic. Previous applications of the END theory to protons colliding with hydrogen atoms [29], hydrogen molecules [32], helium atoms [33], methane molecules [34], oxygen atoms [35], and water molecules [36] show good agreement with experimental data. Most of this work has been done for collision energies ranging from a fraction of an eV to several tens of eV with some semiclassical corrections, e.g., the Airy approximation [32]. Here we are interested in the keV range of projectile energies, where many interesting processes take place.

In a classical treatment, the differential cross section is given in terms of the impact parameter b and the scattering angle θ as

$$\frac{d\sigma}{d\Omega} = \frac{b}{\sin\theta}\left|\frac{db}{d\theta}\right|. \tag{1}$$

Attention to the precise meaning of Eq. (1) leads to questions of whether quantum effects [37,38] in the differential cross section, such as rainbow angles and forward peak scattering, are important. The rainbow angle appears when the scattering angle is not uniquely related to the impact parameter as is assumed in the construction of Eq. (1), thus leading to interference in the differential cross section due to the contribution of two or more distinct trajectories to scattering into the same angle [38]; something not possible to describe classically. The consequences of such interference for the differential cross section has been analyzed previously in the literature [38,39]. The semiclassical treatment using the Airy approximation [40] cures the divergent behavior at the rainbow angle, when it is not too close to zero scattering angle. Another problem needing attention is that the classical treatment of scattering always fails at small scattering angles [37], and a proper description of the cross section in this regime therefore requires a semiclassical or complete quantum treatment. This problem is better treated by the Schiff approximation [41], which takes into account the interference effect.

In Sec. II we give an overview of the theoretical implementation of the END theory used here. In Sec. III we discuss the semiclassical corrections necessary to treat small angle scattering in the keV regime. Section IV contains the details of the calculations. Section V present the results for the direct differential cross sections and their comparison with the available experimental data, and Sec. VI contains the conclusions.

II. ELECTRON-NUCLEAR DYNAMICS THEORY

Since the full details of the method, including the detailed derivation and interpretation of the END equations, have been reported elsewhere (see Refs. [26,31]), we give here only a brief account of the most important features of the theory. The simplest level of the END theory employs a wave function

$$|\psi\rangle = |z,R\rangle|R,P\rangle = |z\rangle|\phi\rangle, \tag{2}$$

where

$$|R,P\rangle = \prod_k \exp\left[-\frac{1}{2}\left(\frac{X_k - R_k}{a_k}\right)^2 + iP_k(X_k - R_k)\right] \tag{3}$$

is the nuclear wave function with R_k and P_k denoting the components of the average position and momentum of a nucleus, respectively, and where

$$|z,R\rangle = |z\rangle = \det\{\chi_i(x_j)\}. \tag{4}$$

is a complex, spin unrestricted, electronic determinantal wave function, which is built from dynamical spin orbitals

$$\chi_i = \phi_i + \sum_{j=N+1}^{K} \phi_j z_{ji}, \quad i = 1,2,\ldots,N. \tag{5}$$

These spin orbitals are expressed in terms of a basis of atomic spin orbitals $\{\phi_i\}$ of rank K, formed from Gaussians centered on the average nuclear position of the dynamically moving nuclei. Forming the quantum mechanical Lagrangian in the limit of zero width parameters $\{a_k\}$ and using the principle of least action produces a set of dynamical equations that govern the time evolution of the dynamical variables $\{z,R,P\}$. This means that the nuclei are treated as classical particles. It is important to note that the dynamics in this form is treated in a laboratory Cartesian system of coordinates and thus circumvents the problem of choosing internal coordinates. The fact that the overall translation and rotational degrees of freedom are included causes no problem since the dynamical equations satisfy general total linear and angular momentum invariance properties.

The END dynamical equations can be expressed in matrix form as

$$\begin{pmatrix} \mathbf{0} & -i\mathbf{C}^* & -i\mathbf{C}_\mathbf{R}^* & \mathbf{0} \\ i\mathbf{C} & \mathbf{0} & i\mathbf{C}_\mathbf{R} & \mathbf{0} \\ i\mathbf{C}_\mathbf{R}^\dagger & -i\mathbf{C}_\mathbf{R}^\mathbf{T} & \mathbf{C}_{\mathbf{RR}} & -\mathbf{I} \\ \mathbf{0} & \mathbf{0} & \mathbf{I} & \mathbf{0} \end{pmatrix} \begin{pmatrix} \dot{\mathbf{z}} \\ \dot{\mathbf{z}}^* \\ \dot{\mathbf{R}} \\ \dot{\mathbf{P}} \end{pmatrix} = \begin{pmatrix} \partial E/\partial \mathbf{z} \\ \partial E/\partial \mathbf{z}^* \\ \partial E/\partial \mathbf{R} \\ \partial E/\partial \mathbf{P} \end{pmatrix}. \tag{6}$$

Here $\dot{\mathbf{z}} = d\mathbf{z}/dt$ and $E = \Sigma_l P_l^2/2M_l + \langle z,R|H_{el}|z,R\rangle$ is the total energy of the system with M_l a nuclear mass, and $H_{\rm el}$ the electronic Hamiltonian including the nuclear-nuclear repulsion. The nonadiabatic coupling terms between electrons and nuclei are expressed in terms of the elements of the dynamical metric on the left of Eq. (6). In particular

$$C_{ph;qg} = \frac{\partial^2 \ln S(z^*,R,z,R')}{\partial z_{ph}^* \partial z_{qg}}\Big|_{R'=R}, \tag{7}$$

$$(C_{X_{ik}})_{ph} = \frac{\partial^2 \ln S(z^*,R,z,R')}{\partial z_{ph}^* \partial X_{ik}}\Big|_{R'=R}, \tag{8}$$

$$(C_{XY})_{ij;kl} = -2\ \mathrm{Im}\frac{\partial^2 \ln S(z^*,R,z,R')}{\partial X_{ij} \partial Y_{kl}}\Big|_{R'=R} \tag{9}$$

are defined in terms of the overlap $S = \langle z,R'|z,R\rangle$ of the determinantal states of two different nuclear configurations. In somewhat more detail, from Eq. (6) one can write

$$i\mathbf{C}\dot{\mathbf{z}} + \sum_l \mathbf{C}_{\mathbf{R}_l}\dot{\mathbf{R}}_l = -i\frac{\partial E}{\partial \mathbf{z}^*} \tag{10}$$

$$-\dot{\mathbf{P}}_k - 2\ \mathrm{Im}\ \mathrm{Tr}\,\mathbf{C}_{\mathbf{R}_k}^\dagger \dot{\mathbf{z}} + \sum_l \mathbf{C}_{\mathbf{R}_k\mathbf{R}_l}\dot{\mathbf{R}}_l = \nabla_{\mathbf{R}_k} E \tag{11}$$

and

$$\dot{\mathbf{R}}_l = \frac{\mathbf{P}_l}{M_l}, \tag{12}$$

where the last equation is purely classical, and where the detailed coupling of the electronic and nuclear degrees of freedom is clearly discernible. This, the simplest of END approximation, can be labeled time-dependent Hartree-Fock (TDHF) for electrons and narrow wave packet nuclei. This approximation is implemented in the ENDyne code [42].

III. DIFFERENTIAL CROSS SECTION: THEORY

The overall features of the differential cross section may be determined by considering the deflection function, whose general shape can be understood from the nature of the projectile-target interaction. However, it is well known that the classical treatment of heavy-particle scattering always fails at sufficiently small angles [37], so analysis of small angle contributions cannot be done purely classically. This is in part because, in a classical collision, the differential cross section, as given by Eq. (1), has two contributions, $d\theta/db$ and $\sin\theta$ in the denominator, that both go to zero as θ does

such that the expression diverges. This problem involves the so called forward-peaked character of the differential cross section.

Thus, for small angles quantum corrections to the differential cross section are needed. In particular, those effects come from the quantum behavior of the nuclear dynamics. In order to account for them in the END theory, we proceed to make a semiclassical approximation.

Let us consider a process in which an atomic projectile with initial velocity v_0, mass M_1, N_1 bound electrons, and nuclear charge $Z_1 e$ collides with a stationary target. The projectile is deflected into the solid angle element $d\Omega$ along a direction with polar angle θ and azimuthal angle φ, measured in the laboratory frame. The Schrödinger equation for the system is given by

$$\left\{ \frac{-\hbar^2}{2M_1}\nabla^2 + \mathbf{H}_1 + \mathbf{H}_2 + V \right\} |\psi\rangle = E|\psi\rangle, \tag{13}$$

where $\mathbf{H}_1$ is the Hamiltonian for the electronic structure of the projectile, $\mathbf{H}_2$ is the Hamiltonian for the electrons plus nuclei of the target, V is the interaction potential for the projectile-target system, and E the total energy. The wave function $|\psi\rangle$ is given by Eq. (2) but in this case, we separate explicitly the functional form for the nuclear motion of the projectile, i.e. [see Eqs. (2) and (3)],

$$\begin{aligned} |\psi\rangle &= |z\rangle|\overline{\phi}\rangle|\phi_1\rangle \\ &= |\overline{\psi}\rangle|\phi_1\rangle. \end{aligned} \tag{14}$$

The only difference with Eq. (3) is that now, the projectile is described by a quantum wave function. Substituting Eq. (14) in Eq. (13), rearranging, and projecting over a specific state s, we obtain the Schrödinger wave equation for the scattered projectile as

$$\{\nabla^2 + k_s^2\}|\phi_1\rangle = U_s|\phi_1\rangle, \tag{15}$$

where

$$U_s = \frac{2M_1}{\hbar^2}\langle\overline{\psi}_s|V|\overline{\psi}\rangle/\langle\overline{\psi}_s|\overline{\psi}\rangle \tag{16}$$

is the screened interaction potential, and $k_s^2 = (2M_1/\hbar^2)(E - E_1 - E_2)$, the momentum of the projectile during the collision with $E_1 = \langle\overline{\psi}_s|\mathbf{H}_1|\overline{\psi}\rangle/\langle\overline{\psi}_s|\overline{\psi}\rangle$ and $E_2 = \langle\overline{\psi}_s|\mathbf{H}_1|\overline{\psi}\rangle/\langle\overline{\psi}_s|\overline{\psi}\rangle$. The solution to the inhomogeneous Eq. (15) corresponding to outgoing spherical waves is given by

$$\begin{aligned} |\phi_1\rangle &\to e^{i\mathbf{k}_0\cdot\mathbf{R}_1}\delta_{0s} - \frac{e^{ik_sR_1}}{4\pi R_1}\int e^{-i\mathbf{k}_s\cdot\mathbf{R}_1'}U_s(\mathbf{R}_1')|\phi_1\rangle d\mathbf{R}_1' \\ &\to e^{i\mathbf{k}_0\cdot\mathbf{R}_1}\delta_{0s} + \frac{e^{ik_sR_1}}{R_1}f(\mathbf{k}_s,\mathbf{k}_0). \end{aligned} \tag{17}$$

Here, $\mathbf{k}_0$ is a vector of magnitude k_0 along the direction of incidence, $\mathbf{k}_s$ is a vector of magnitude k_s along the direction of observation, and where $f(\mathbf{k}_s,\mathbf{k}_0)$ is the scattering amplitude. As is well known, applying Eq. (17) recursively one obtains the infinite Born series

$$\begin{aligned} f(\mathbf{k}_s,\mathbf{k}_0) = -\frac{1}{4\pi}\sum_{n=1}^{\infty}\int\cdots\int e^{-i\mathbf{k}_s\cdot\mathbf{R}_n}U_s(\mathbf{R}_n) \\ \times G(\mathbf{R}_n-\mathbf{R}_{n-1})U_s(\mathbf{R}_{n-1}) \\ \times G(\mathbf{R}_{n-1}-\mathbf{R}_{n-2})\cdots U_s(\mathbf{R}_2) \\ \times G(\mathbf{R}_2-\mathbf{R}_1)U_s(\mathbf{R}_1)e^{i\mathbf{k}_0\cdot\mathbf{R}_1}d\mathbf{R}_1\cdots d\mathbf{R}_n, \end{aligned} \tag{18}$$

where G is the outgoing wave Green's function for the operator $(\nabla^2 + k_s^2)$

$$G(\rho) = -\frac{1}{4\pi\rho}e^{ik_s\rho}. \tag{19}$$

The first term of the series yield the usual first Born approximation; higher terms are very laborious to calculate, unless approximations are made.

In order to take in account all the Born terms, we will apply the Schiff approximation [41] which consist in summing Eq. (18) after approximating each term by the method of stationary phase. This method is valid for large k. Following a procedure similar to that of Schiff for small scattering angles, θ, where the only difference in the analysis is the interaction potential [Eq. (16)], the following result is obtained:

$$f(\theta) = ik\int_0^{\infty}\{1-\exp[-2i\zeta(b)]\}J_0(qb)bdb, \tag{20}$$

for the scattering amplitude, where $q = |\mathbf{k}_s - \mathbf{k}_0|$ is the momentum transfered during the collision, θ is the angle between $\mathbf{k}_s$ and $\mathbf{k}_0$ (scattering angle), and

$$\zeta(b) = \frac{1}{4k}\int_{-\infty}^{\infty}U_s(b,x)dx, \tag{21}$$

with $J_0(x)$ the Bessel function of order zero. When only elastic processes are considered, $q = 2k\sin(\theta/2)$ with k being the initial wave vector of the projectile. According to Mason *et al.* [37], $\zeta(b)$ is just the negative of the semiclassical phase shift $\delta(b)$. In addition, the semiclassical phase shift is related to the deflection function through [43,38]

$$\Theta(b) = \frac{2}{k}\frac{d\delta(b)}{db}. \tag{22}$$

Therefore, Eq. (20) is the semiclassical expression for the scattering amplitude.

From Eq. (17) we obtain the probability for the particle being scattered in a direction $\mathbf{k}_s$, when divided by the incoming flux, it determines the differential cross section as [43]

$$\frac{d\sigma}{d\Omega} = \frac{k_s}{k_0}|f(\theta)|^2. \tag{23}$$

From this expression one sees that once the deflection function is determined and the probability for the exit channel is known, the differential cross section is established. For the case of direct scattering, we have that $|\overline{\psi_s}\rangle = |\overline{\psi}\rangle$, i.e. we consider all the exit channels. In the next section we describe the procedure for determining the deflection function and the differential cross section, in the END formalism.

IV. DETAILS OF THE CALCULATIONS

We consider swift protons, hydrogen atoms, and helium atoms, at energies of 0.5, 1.5, and 5.0 keV as projectiles impinging on helium or neon atom gas targets. The target atom is placed at the origin in a Cartesian laboratory system and the projectile is traveling towards the target with an initial velocity along the x axis and with an impact parameter b along the y axis. We set initially the projectile at 30 a.u. away from the target and make it collide, stopping the dynamics after the projectile is again at 30 a.u. away from the target.

For helium, we use a VDZ (valence double zeta) $[4s1p]$ uncontracted basis set [44]. For protons and hydrogen atoms we employ a pVDZ (polarized VDZ) $[4s1p/2s1p]$ [45], while for neon we use a SV (single valence) $[10s5p/3s2p]$ basis set [46] which also are uncontracted.

To accurately represent the continuum a large basis is required. The details of the transition are not as critical for the differential cross section as they are for energy loss (ΔE), stopping power $(-dE/dx)$, and state to state total cross section calculations, as long as the overall transition space is well represented [47]. A method to describe ionization processes explicitly by using basis functions that move freely in space as determined by electronic dynamics has been developed and coded [48]. This method has not been used in this work (see Sect. V B below) and its results will be reported in a future publication.

The END approach uses a ''supermolecule'' description of the system, i.e., a single spin unrestricted determinantal wave function is used to describe the system electrons as a whole expressed in a basis of Gaussian orbitals centered on the dynamically changing nuclear positions. For each impact parameter value from $b=0.0$ (head-on collision) to $b=10.0$ a.u. in steps of 0.01 a.u., we calculate the angle of deflection of the projectile, $\Theta(b)$ (the deflection function), the final projectile charge, and the final energy (nuclear kinetic energy, and internal energy) for the projectile. Once we have the deflection function, the absolute differential cross section is obtained by means of Eq. (23) where the scattering amplitude $f(\theta)$ is derived via a semiclassical approximation and where $\hbar k_0$ and $\hbar k_s$ are the initial and final momenta of the projectile, respectively.

V. RESULTS

In Fig. 1, we show the deflection function for 0.5 keV protons and hydrogen colliding with neutral helium. The minimum in the deflection function defines the rainbow angle, while the crossing from one branch to another is called the glory angle. While the deflection function for hydrogen atom projectiles is monotonically decreasing for increasing impact parameters, proton projectiles on the same target produce a deflection function that goes through a minimum. For small impact parameter $(b<1.0)$ the proton-helium interaction is repulsive, while for $b>1.0$ the collision is attractive. This is due to the electronic structure of the system and the repulsion stems from the nuclear-nuclear interaction when the proton penetrates the helium electron cloud.

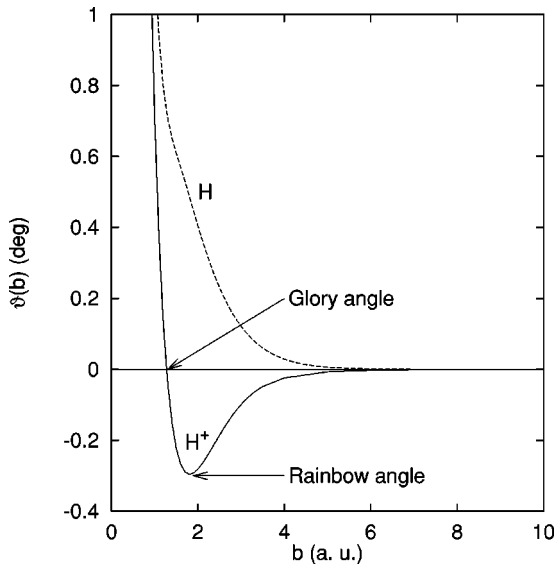

FIG. 1. Deflection function $\Theta(b)$ for protons and hydrogen projectiles at 0.5 keV incident on atomic He.

The results from the theoretical determination of the rainbow angle as given by the minimum of the deflection function of protons colliding with ground state helium atoms at different energies are listed in Table I. The END results agree well with the experimental values determined by Johnson *et al.* [49].

A. Differential cross section

Once the deflection function is determined, the differential cross section is obtained from the application of Eqs. (23) and (20). In the following we show the direct cross sections for a number of different collisional systems at 0.5, 1.5, and 5.0 keV. The theoretical cross sections determined from END are given in a solid line and in the same graph the experimental results are displayed with open circles or error bars if they are available.

TABLE I. Rainbow angle (deg) for H^+ on He.

Energy (keV)	END	Experiment[a]
0.5	0.296	0.32
1.5	0.101	0.11
5.0	0.031	0.03

[a]Johnson *et al.* [49].

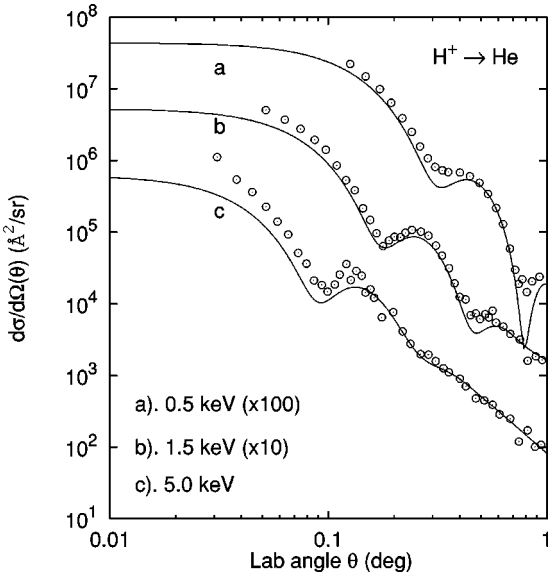

FIG. 2. Comparison of direct differential cross section for H^+ at 0.5, 1.5, and 5.0 keV incident on atomic He. The experimental data are from Johnson *et al.* [49].

In Fig. 2 we show the differential cross sections for protons colliding with neutral helium at 0.5, 1.5, and 5.0 keV for small scattering angles and compare the calculated results with the experimental data of Johnson *et al.* [49].

For neutral hydrogen colliding with helium, there is no rainbow angle, as the deflection function is repulsive for all impact parameters, and thus the differential cross section in Fig. 3 shows no structure in contrast to the case of proton projectiles. The experimental data of Gao *et al.* [50] are used for comparison. Note that for large scattering angles the collision is no longer elastic as the probability for electron excitations is appreciable at these angles, since (see Fig. 1) large angles correspond to small impact parameters. In this case the deflection function carries information concerning inelastic properties of the collision, such as electron transfer and electronic excitations. In the same figure we show the differential cross section (dashed line) for elastic collisions when the projectile leaves in the ground state. This is obtained by projecting the final state wave function of the projectile into the ground state expressed in the same basis set. The projected results clearly shows the contributions of the excitation for large angles and high energies.

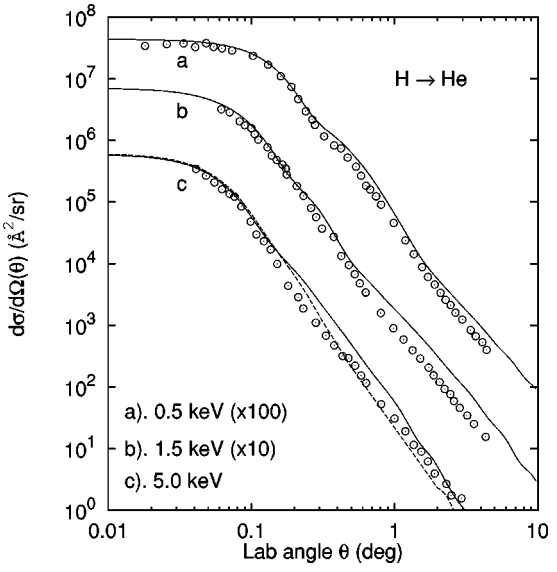

FIG. 3. Comparison of direct differential cross section for H projectiles at 0.5, 1.5, and 5.0 keV incident on atomic He. The experimental data are from Gao *et al.* [50]. Also, we show the differential cross section for elastic scattering (dashed line) for projectiles at 5.0 keV leaving in the ground state. See text.

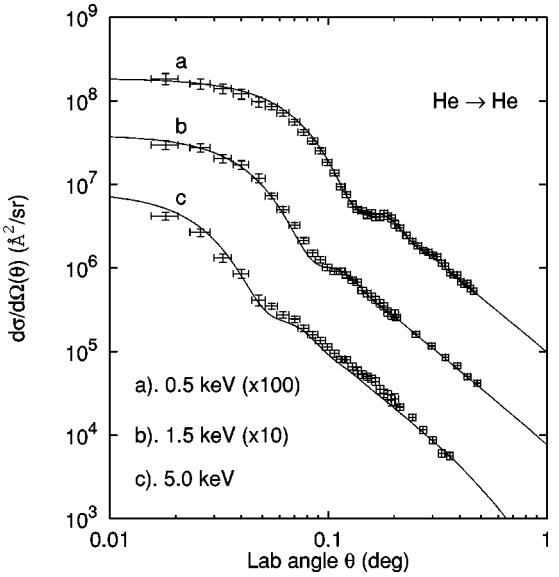

FIG. 4. Direct differential cross section for helium projectiles at 0.5, 1.5, and 5.0 keV incident on atomic helium targets. The experimental data are from Nitz *et al.* [12].

In Fig. 4, we show the direct differential cross section for helium projectiles colliding with neutral helium. The results

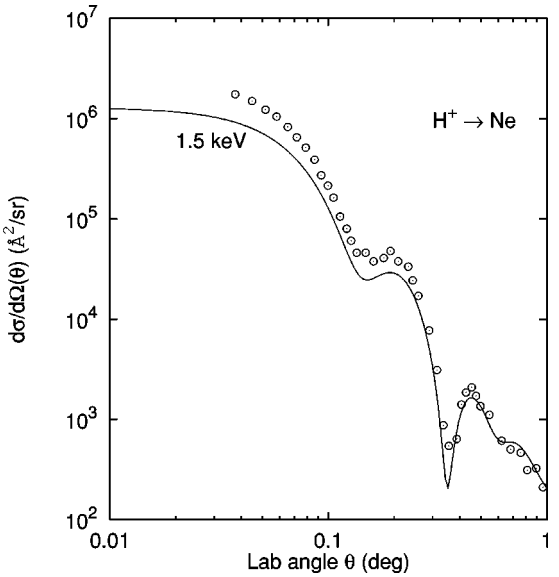

FIG. 5. Direct differential cross section for protons projectiles at 1.5 keV incident on atomic neon targets. The experimental results are from Johnson *et al.* [51]

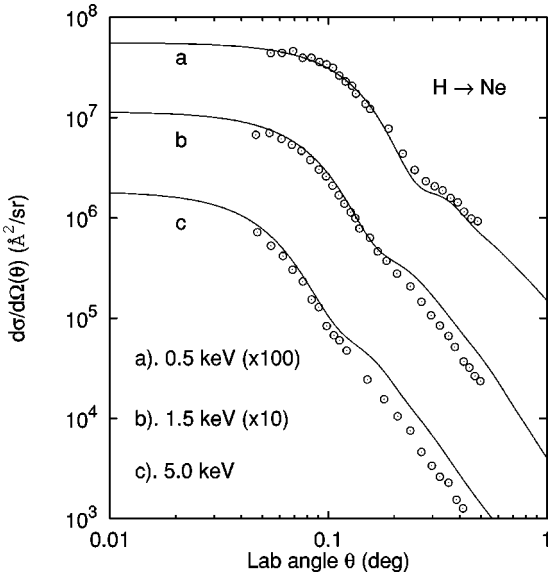

FIG. 6. Direct differential cross section for hydrogen projectiles at 0.5, 1.5, and 5.0 keV incident on atomic neon targets. The experimental results were taken from Gao *et al.* [50]

TABLE II. Absolute integral cross section in Å^2.

Process	END	Experiment	Angular range
$H^+ \rightarrow He(0.5\ keV)$	6.31	7.2 [a]	$0.08° - 1.2°$
$H^+ \rightarrow He(1.5\ keV)$	2.99	4.0 [a]	$0.04° - 0.882°$
$H^+ \rightarrow He(5.0\ keV)$	1.51	2.3 [a]	$0.02° - 1.0°$
$H \rightarrow He(0.5\ keV)$	12.17	11.0 ± 0.6 [b]	$0.018° - 4.5°$
$H \rightarrow He(1.5\ keV)$	7.25	4.4 ± 0.2 [b]	$0.05° - 4.5°$
$H \rightarrow He(5.0\ keV)$	2.75	1.5 ± 0.8 [b]	$0.05° - 4.5°$
$He \rightarrow He(0.5\ keV)$	10.12		$0.018° - 0.5°$
$He \rightarrow He(1.5\ keV)$	8.98		$0.018° - 0.5°$
$He \rightarrow He(5.0\ keV)$	6.57		$0.018° - 0.5°$
$H \rightarrow Ne(0.5\ keV)$	9.87	10.0 ± 0.5 [b]	$0.05° - 0.5°$
$H \rightarrow Ne(1.5\ keV)$	8.39	7.0 ± 0.4 [b]	$0.05° - 0.5°$
$H \rightarrow Ne(5.0\ keV)$	4.44	3.1 ± 0.2 [b]	$0.05° - 0.5°$
$He \rightarrow Ne(0.5\ keV)$	8.23		$0.05° - 0.5°$
$He \rightarrow Ne(1.5\ keV)$	5.41		$0.05° - 0.5°$
$He \rightarrow Ne(5.0\ keV)$	4.58		$0.05° - 0.5°$

[a]Johnson *et al.* [49].
[b]Gao *et al.* [50].

for small angles are compared with the experimental data of Nitz *et al.* [12].

Up to this point we have shown results for simple systems with no more than two to four electrons. The END approach is general and we should be able to use more complex targets and projectiles. In Fig. 5, we display the direct differential cross section for proton projectiles at 1.5 keV incidents on neutral neon and compare them with the experimental data of Johnson *et al.* [51], and in Fig. 6 we show the differential cross section for hydrogen atom projectiles colliding on the same target at 0.5, 1.5, and 5.0 keV, and compared with the experimental data of Gao *et al.* [50].

In Fig. 7, the differential cross sections for helium projectiles colliding with neon atoms at 0.5, 1.5, and 5.0 keV are displayed, and compared with the experimental data of Gao *et al.* [52].

Once we have obtained the differential cross section, the total cross section is obtained through an angular integration. In Table II we give the calculated total cross section integrated over all the experimental angular region and compare with the experimental data available [49,50]. Again we see a good agreement with the experimental data.

B. Projectile charge state

In Fig. 8 we show the final Mulliken population [53] as a measure of the electronic charge distribution for protons, hy-

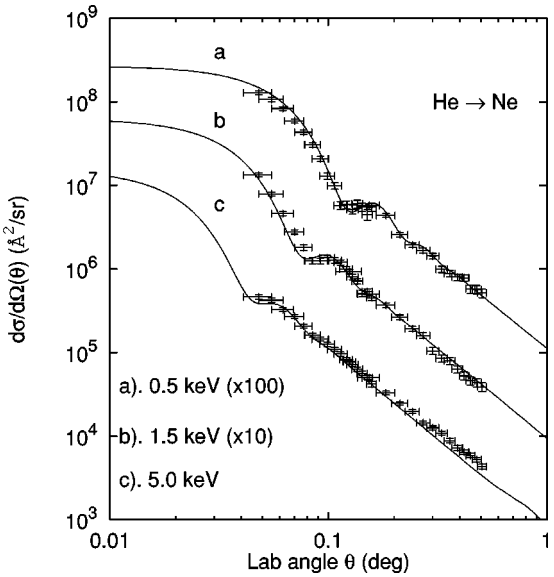

FIG. 7. Direct differential cross section for helium projectiles at 0.5, 1.5, and 5.0 keV incident on atomic neon. The experimental results are from Gao *et al.* [52].

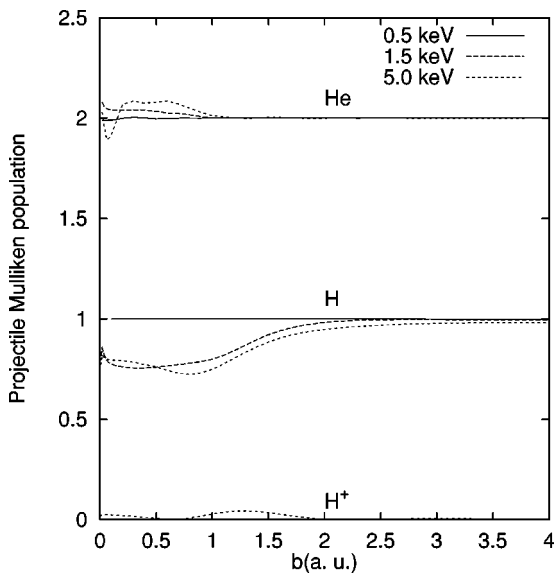

FIG. 8. Final electron charge (Mulliken population) for protons, H and He projectiles at 0.5, 1.5, and 5.0 incident on helium targets as a function of the impact parameter.

drogen, and helium projectiles as a function of the impact parameter b, after the interaction with helium targets. The electron transfer is the difference of the Mulliken population and the initial number of electrons on the projectile. From this figure one notes that the probability for electron transfer for protons and helium is very low, and increases for higher projectile energies. In view of the high ionization potential for helium (~ 24 eV), ionization processes are negligible at these collision energies. For example, protons at 5.0 keV colliding with He, the ionization cross section is 0.01 Å^2 [54], which is 0.5% of the value reported in this work. However, electron transfer is more likely for small impact parameters where the interaction is stronger. This makes the collision mostly elastic for $b > 1.0$ a.u. On the other hand, for hydrogen projectiles we see from Fig. 8 that for low impact parameters the electron transfer is higher than for protons. The reason is that the ionization potential of hydrogen is lower than that for helium, making it share electronic charge with the target. Also, the hydrogen projectile is more easily excited electronically, making the collision effectively inelastic. This is more pronounced for small impact parameters (greater scattering angles) and higher energies, as expected.

This behavior has implications for the structure of the differential cross section, since these processes are no longer elastic in the region of larger scattering angles. This effect can be noted in Figs. 3 and 6 in the low impact parameter region (large scattering angle), where the experimental cross sections are purportedly elastic, since the setup [50] ensures that only elastic processes are counted.

VI. CONCLUSIONS

We have shown that the electron nuclear dynamics theory in its simplest implementation with suitable semiclassical corrections is capable of yielding differential and integral cross sections in excellent agreement with the experiments. In addition this supermolecular theoretical approach can also yield dynamical charge exchange.

In this work we have concentrated on direct scattering processes, but the END method allows one to study state to state process as for example, excitations, ionizations and energy loss. Since these processes are strongly dependent on the completeness of the basis set, they require somewhat more extensive analysis. This work is in progress.

ACKNOWLEDGMENTS

One of us (R.C.T.) thanks CONACyT-Mexico for its support, which made his stay at the University of Florida possible. This work is supported partially by NSF (Grant No. CHE-9732902), ONR (Grant No. N0014-97-1-0261), and IBM (SUR 1999). This support is gratefully acknowledged.

[1] T. Ishihara and J.H. McGuire, Phys. Rev. A **38**, 3310 (1988).
[2] M. Kimura and C.D. Lin, Phys. Rev. A **34**, 176 (1986).
[3] J. Burgdörfer and L.J. Dubé, Phys. Rev. Lett. **52**, 2225 (1984).
[4] N. Shimakura, H. Sato, M. Kimura, and T. Wanatabe, J. Phys. B **20**, 1801 (1987).
[5] A. Jain, C.D. Lin, and W. Fritsch, J. Phys. B **21**, 1545 (1988).
[6] W. Fritsch and C.D. Lin, J. Phys. B **19**, 2683 (1986).
[7] J.B. Delos, Rev. Mod. Phys. **53**, 287 (1981).
[8] M. Kimura and N. F. Lane, in *Advances in Atomic, Molecular and Optical Physics*, edited by D. Bates and B. Bederson (Academic Press, New York, 1980).
[9] A. Riera, in *Time-Dependent Quantum Molecular Dynamics*, edited by J. Broeckhove and L. Lathouwers (Plenum, New York, 1992).
[10] F.T. Smith, Phys. Rev. **179**, 111 (1969).
[11] L. Wilets and S.J. Wallace, Phys. Rev. **169**, 169 (1968).
[12] D.E. Nitz *et al.*, Phys. Rev. A **35**, 4541 (1987).
[13] G. Schiwietz, Phys. Rev. A **42**, 296 (1990).
[14] J. Macek and C. Wang, Phys. Rev. A **34**, 1787 (1986).
[15] D.R. Schultz, J.C. Wells, P.S. Krstić, and C.O. Reynhold, Phys. Rev. A **56**, 3710 (1997).
[16] D.R. Schultz, M.R. Strayer, and J.C. Wells, Phys. Rev. Lett. **82**, 3976 (1999).
[17] B.M. Deb, P.K. Chattaraj, and S. Mishra, Phys. Rev. A **43**, 1248 (1991).
[18] B.M. Deb and P.K. Chattaraj, Phys. Rev. A **39**, 1696 (1985).
[19] R. Car and M. Parrinello, Phys. Rev. Lett. **55**, 2471 (1985).
[20] D.K. Remler and P.A. Madden, Mol. Phys. **70**, 921 (1990).
[21] M.C. Payne *et al.* Rev. Mod. Phys. **64**, 1045 (1992).
[22] J. Theilhaber, Phys. Rev. B **46**, 12 990 (1992).
[23] K.C. Kulander, K.R. Sandhya, and S.E. Koonin, Phys. Rev. A **25**, 2968 (1982).
[24] D.H. Tiszauer and K.C. Kulander, Comput. Phys. Commun. **63**, 351 (1991).
[25] D. A. Micha and K. Runge, in *Time-Dependent Quantum Molecular Dynamics*, edited by J. Broeckhove and L. Lathouwers (Plenum, New York, 1992).
[26] E. Deumens, A. Diz, R. Longo, and Y. Öhrn, Rev. Mod. Phys. **66**, 917 (1994).
[27] K.J. Schaudt, N.H. Kwong, and J.D. Garcia, Phys. Rev. A **43**, 2294 (1991).
[28] E. Deumens and Y. Öhrn, J. Phys. Chem. **92**, 3181 (1988).
[29] E. Deumens, A. Diz, H. Taylor, and Y. Öhrn, J. Chem. Phys. **96**, 6820 (1992).
[30] Y. Öhrn *et al.*, in *Time-Dependent Quantum Molecular Dynamics*, edited by J. Broeckhove and L. Lathouwers (Plenum, New York, 1992), pp. 279–292.
[31] E. Deumens and Y. Öhrn, J. Chem. Soc., Faraday Trans. **93**, 919 (1997).
[32] J.A. Morales, A.C. Diz, E. Deumens, and Y. Öhrn, J. Chem. Phys. **103**, 9968 (1995).
[33] R. Longo, E. Deumens, and Y. Öhrn, J. Chem. Phys. **99**, 4554 (1993).
[34] D. Jacquemin, J.A. Morales, E. Deumens, and Y. Öhrn, J. Chem. Phys. **107**, 6146 (1997).
[35] M. Hedström, E. Deumens, and Y. Öhrn, Phys. Rev. A **57**, 2625 (1998).
[36] M. Hedström, J.A. Morales, E. Deumens, and Y. Öhrn, Chem. Phys. Lett. **279**, 241 (1997).

[37] E.A. Mason, J.T. Vanderslice, and C.J.G. Raw, J. Chem. Phys. **40**, 2153 (1964).
[38] K.W. Ford and J.A. Wheeler, Ann. Phys. (N.Y.) **7**, 259 (1959).
[39] M.V. Berry, Proc. Phys. Soc. London **89**, 479 (1966).
[40] D. M. Brink, *Semi-classical Methods in Nucleus-nucleus Scattering* (Cambridge University press, New York, 1985).
[41] L.I. Schiff, Phys. Rev. **103**, 443 (1956).
[42] E. Deumens *et al.*, ''ENDyne version 2.7 Software for Electron Nuclear Dynamics, Quantum Theory Project, University of Florida, 1998.
[43] N. F. Mott and H. S. W. Massey, *The Theory of Atomic Collisions*, 3rd ed. (Clarendon Press, Oxford, 1965).
[44] A. Schafer, H. Horn, and R. Ahlrichs, J. Chem. Phys. **97**, 2571 (1992).
[45] T.H. Dunning, J. Chem. Phys. **90**, 1007 (1989).
[46] T. H. Dunning and P. J. Hay, in *In Methods of Electronic Structure Theory*, edited by H. F. Schaefer III (Plenum Press, New York, 1977), Vol. 2.
[47] R. Cabrera-Trujillo, J. R. Sabin, E. Deumens, and Y. Öhrn (unpublished).
[48] B. Mogensen, in *A Novel Approach to Electron Molecule Reactions*, Ph. D. thesis (Copenhagen University, Denmark, 1997).
[49] L.K. Johnson *et al.*, Phys. Rev. A **40**, 3626 (1989).
[50] R.S. Gao, L.K. Johnson, K.A. Smith, and R.F. Stebbings, Phys. Rev. A **40**, 4914 (1989).
[51] L.K. Johnson *et al.*, Phys. Rev. A **40**, 4920 (1989).
[52] R.S. Gao *et al.*, Phys. Rev. A **36**, 3077 (1987).
[53] R.S. Mulliken, J. Chem. Phys. **23**, 1833 (1955).
[54] P.S. Krstić, D.R. Schultz, and G. Bent, J. Phys. B **31**, 183 (1998).